

Research on the Identification Modeling of Air-Magnet Active Vibration Isolation System

Xianglong Wen^{1,a}, Caizhan Zhu¹, Rongli Hu¹, Chunsheng Song¹, Jinguang Zhang¹

¹ School of Mechanical and Electronic Engineering, Wuhan University of Technology, Wuhan, Hubei, China

Abstract. The methods of the identification modeling of air-magnet active vibration isolation system (AMAVIS) are studied. Difference equation model and transfer function model are established respectively in the time domain and frequency domain. The models are analyzed and proved by the experiment. Identification results show that the order of frequency identification is higher than the time identification model. But when it comes to accuracy and convergence, frequency identification model has obvious advantage. This paper provides evidence for subsequent active vibration control. The conclusion is the basic of subsequent experiment and research.

1 Introduction

In a variety of different engineering systems there is a requirement to isolate sensitive equipment from foundation vibration alternatively, isolate the foundation from machinery vibration [1]. As an important elastic element of the air suspension, air spring, has the characteristics of large bearing capacity, small size, low natural frequency which changes a little, and outstanding high frequency anti-vibration performance [2]. Moreover, the magnetic vibration isolator possesses the advantages such as changeable stiffness and damping, fast response, large frequency bandwidth, easy to control and so on [3]. Therefore, active vibration isolation technology, which combines air spring and maglev vibration isolator, can take full advantage of the two kinds of isolator. It realizes vibration control in a wider frequency range, thus, it could be an effective means to reduce vibration. But the combination of the two constitutes a complex system of strong coupling, nonlinear, traditional modeling theory is difficult to accurately describe the system.

Xing J T established a generalized mathematical model for the control equation, and derived a governing equation to describe the interaction between elastic structure and multi-channel electromagnetic excitation and control system [4]. He L adopts an improved FxLMS algorithm for multi channel to reduce the complexity of the calculation and effectively compensate the actuator nonlinearity [5]. A new adaptive active control strategy with online secondary path modeling is proposed and applied in two-stage active vibration isolation system and the results show good vibration reduction and strong robust [6]. Tom Oomen develops a new data-driven H_∞ norm estimation algorithm for model-error modeling of multivariable systems, and the approach is experimentally implemented on an industrial active

vibration isolation system [7]. Deng Xi-shu designs a simulated Vibration-isolation Testing Equipment of the Stepping and Scanning Lithography which the inner-world and the outside-world are connected by four precision six degree of free vibration isolators based on its motion features and working requirements in industry [8].

This paper analyses the identifiability of AMAVIS, establishes difference equation model and transfer function model respectively in the time domain and frequency domain, and verifies the model.

2 System identifiability

The mathematical model, that the system describes, includes parameter model and non parameter model. The parameter model utilizes finite parameter to describe the model in the study, or use the coefficients of the model to describe the system. Non parameter model describe system by response curve. Identification technique provides a means to transform non parameter model into parameter model. It obtains transfer function or frequency response function matrix from response curve by the method of dynamic fitting.

The AMAVIS is illustrated in fig.1. As shown in the figure, signal 1 is acceleration response signal of the target on the steel plate, which has been conditioned and filtered. Filtering signal 6 is DC voltage excitation signal, the control channel model outputs signal 7.

^a Corresponding author: wenxl@whut.edu.cn

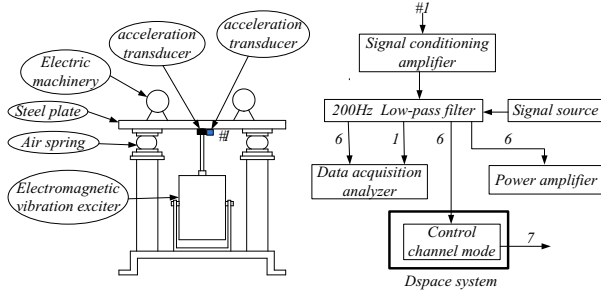


Figure 1. Diagram of System identification model

Fig.2 describes the actual system and its input-output data acquisition, conversion and identification process until obtain the model to describe the relationship between input and output.

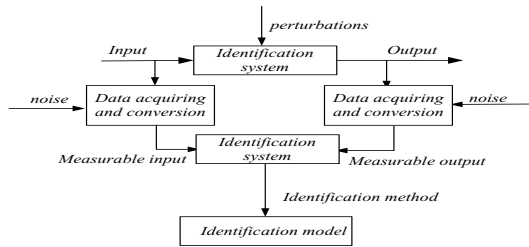


Figure 2. Diagram of the process of identification

In the AMAVIS, the transfer function between the electromagnetic vibrator and control target on the steel plate can be described by the following formula.

$$G(s) = \frac{Y(s)}{U(s)} = \frac{b_0 + b_1s + b_2s^2 + \dots + b_ms^m}{1 + a_1s + a_2s^2 + \dots + a_ns^n} \quad (1)$$

In the formula (1), Y(s) is the Laplace transform of the output response and U(s) is Laplace transform of excitory input. Doing some partial fraction decomposition to formula 1 can obtain the following formula.

$$G(s) = \sum_{i=1}^n \frac{A_i}{s - s_i} \quad (2)$$

s_i is pole of G(s), A_i is the residue which it corresponds to.

The excitation impulse response of corresponding points can be got through inverse Laplace transform from formula (2).

$$h(s) = \sum_{i=1}^n A_i e^{s_i t} \quad (3)$$

Their discrete forms of expression can be got through discrete sampling towards impulse response.

$$h(k) = \sum_{i=1}^n A_i e^{s_i kT} \quad (4)$$

k is the number of sampling points, $k=1,2,3,\dots$, T is the sampling period.

The following formula can get by z-transform.

$$H(z) = \sum_{i=1}^n \frac{A_i}{1 - e^{s_i T} Z^{-1}} \quad (5)$$

The rational fraction form be got obtained by reduction of fractions to a common denominator.

$$H(s) = \frac{b_0 + b_1z^{-1} + b_2z^{-2} + \dots + b_{n-1}z^{-n+1}}{1 + a_1z^{-1} + a_2z^{-2} + \dots + a_nz^{-n}} \quad (6)$$

Formula (6) is the pulse transfer function of dynamic discrete systems. The system it corresponds to is:

$$(1 + a_1z^{-1} + a_2z^{-2} + \dots + a_nz^{-n}) Z\{y(k)\} = (b_0 + b_1z^{-1} + b_2z^{-2} + \dots + b_{n-1}z^{-n+1}) Z\{u(k)\} \quad (7)$$

The following formula can be got by z-transform from formula (6).

$$y(k) + a_1y(k-1) + \dots + a_ny(k-n) = b_0u(k) + b_1u(k-1) + b_2u(k-2) + \dots + b_{n-1}u(k-n+1) \quad (8)$$

Formula (8) reflects relationship between u(k) and y(k). u(k) and y(k) are input and output sampling sequence of dynamic discrete system.

Formula (1) is the basis of the frequency domain identification. The transfer function model parameter identification can be done by processing experimental frequency response data, so as to obtain the transfer function of the system. Formula (8) is the basis of the frequency domain identification. Based on the input and output data of the system in the current time and some time before, the differential equation model of the system can be calculated by a certain identification algorithm.

3 Prior knowledge of the identification system

Multi channel signal acquisition analyzer samples input, output signal and the frequency response signal. Fig.3 shows experimental frequency response. As shown in fig.3, the natural frequency of the system tested in the range of 200Hz is consistent with the results of finite element analysis. The location of the peak point in the amplitude-frequency characteristic curve is broadly consistent with the results of finite element analysis. It proves the reliability of experimental environment.

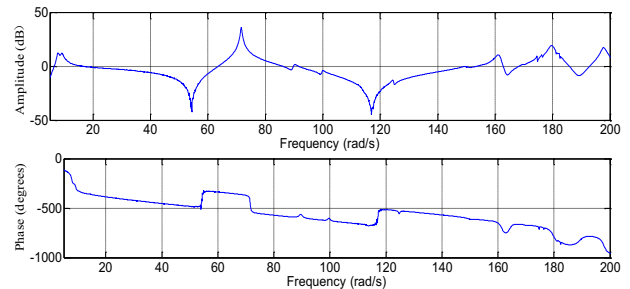


Figure 3. Frequency characteristics of Bode diagram

Moreover, fig.3 also shows that, in the phase-frequency diagram, the overall trend of the phase is decreasing linearly with frequency. Therefore lag time exists in the system and lag time of phase and frequency

is a linear relationship. Make phase change boundaries to determine the lag time constant, just as shown in fig.4.

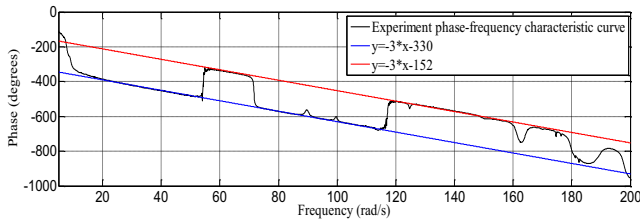


Figure 4. Phase frequency characteristic curves with boundary

Fig.4 shows that the overall trend of the phase is decreasing linearly with frequency. Control channel exists lag time. Suppose that the transfer function of lag time is: $G_1(s) = e^{-\tau s}$. The phase frequency characteristic is: $\varphi(\omega) = -\tau\omega$. As the fig.5 shows, $-\pi\tau/\pi \cdot 180 \approx -3.0$, $\tau \approx 0.0083$.

Vertical difference between the two curves in fig.5 is 178, that is to say, the phase change in the range of 180 degree range. The resonance and anti resonance point can be regarded as the two order links. The acceleration sensor is used in the model and the control channel also contains a second-order differential link.

4 Analysis and identification of model

The data collected for the model was processed in MATLAB. The order of time domain identification model is identified as 13 and the order of the frequency model as 18.

Fig.5 is the amplitude frequency characteristics obtained by two kinds of identification methods. The figure shows that several major peaks in experimental data are fitted out from frequency domain identification model, while the time-domain model fitting result is slightly worse.

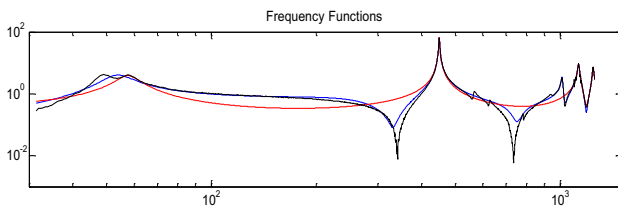


Figure 5. The amplitude frequency characteristic curve

Fig.6 is the pole distribution of the transfer function model. The figure shows that the poles are all located in the unit circle and the model is stable.

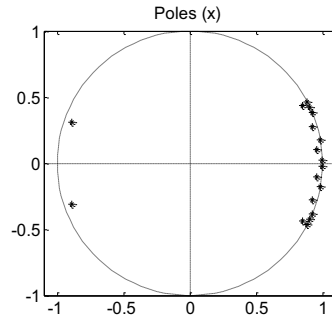


Figure 6. Pole distribution chart

In conclusion, order obtained from frequency identification is higher than the order obtained from time domain identification model, but frequency domain identification model is superior to the accuracy and convergence. Irrespective of the difficulty of controller design, priority should be given to the frequency domain identification model as a model of AMAVIS of single-input and single-output control channel.

In this paper, frequency domain identification model is used to describe AMAVIS. Characteristic curves obtained from frequency domain identification model and experiment is shown in the Fig.7.

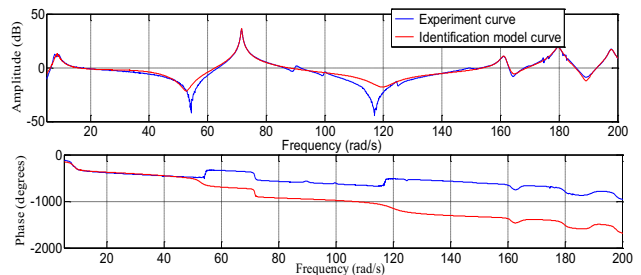


Figure 7. The frequency characteristic curve of experiment and model

From Fig.7 can know that:

(1) Maxima are fitted out in the amplitude-frequency characteristic diagram, while the minimum fit is not very good, but the overall shape of the two curves is not very different.

(2) Phase frequency characteristics of the phase diagram will have large changes in the resonance frequency and anti-resonance frequencies, but there are differences in the direction of change. In the anti-resonance frequency, the phase of the experimental curve is upward mutation, but the model curve is downward mutation. At the resonance frequency, the phase of the two curves is downward mutation.

5 Validation of the identification model

Take the following methods to validate whether frequency domain identification model identified appropriately expresses the identification system. As shown in the fig.1, the excitation signal is simultaneously applied to the actual system and input into the frequency domain identification model identified. Then the actual output data of the system and the identification model are

obtained. The real-time experimental frequency response curve and frequency response curve of the model are shown in the fig.8.

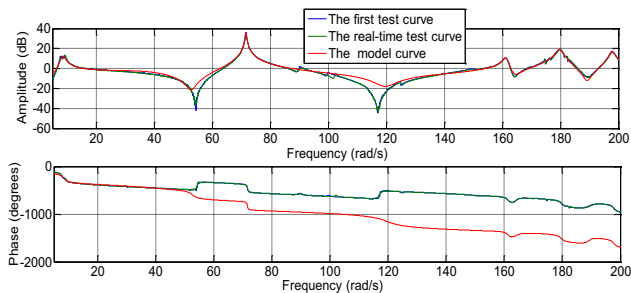


Figure 8. The model validation frequency response chart

In the time domain, fig.9 shows the input excitation signal, the experimental output signal and the model output signal.

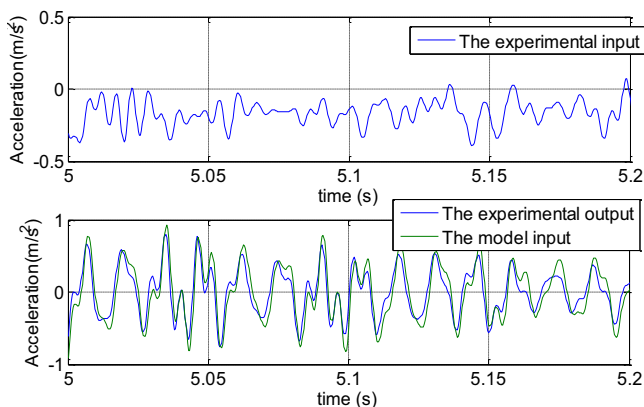


Figure 9. The model validation time response chart

Fig.8-9 shows that, no matter in the time domain or frequency domain, identification model and actual model has good consistency. In the frequency domain, identification model gets a high precision fit on amplitude-frequency characteristics peak of the system. In addition, the model output always can follow experimental output. That means identification model has relatively high precision. In other words, it can accurate describe the system identified.

6 Conclusions

Given the complexity and accuracy of AMAVIS, in this paper, the experimental identification modeling is used to describe the system. It provides evidence for subsequent active vibration control. On the basis of the analysis on the identifiability of the system, identification modeling was carried out in time domain and frequency domain. Identification results show that the order of frequency identification is higher than the time identification model. But when it comes to accuracy and convergence, frequency identification model has obvious advantage.

Acknowledgements

The research work was supported by National Natural Science Foundation of China under Grant No. 51205296 and 51275368.

References

1. S. Daley, J. Hätönen, D.H. Owens. Active vibration isolation in a smart spring mounts using a repetitive control approach. *Control Engineering Practice*. 2006, 14(9): 991-997
2. Kim H, Kim C, Choi S, et al. Triple mechanism of an active air spring combining pneumatics, electromagnets and MR fluid in an air mount. Vilnius, Lithuania: International Institute of Acoustics and Vibrations, 2012. 1381-1388
3. Ning D, Sun C. Study on active vibration isolation based on electromagnetic responses. Zhangjiajie, China: 2012. 648-652.
4. Xing J T, Xiong Y P, Price W G. A generalized mathematical model and analysis for integrated multi-channel vibration structure-control interaction systems. *Journal of Sound and Vibration*, 2009, 320(3): 584-616.
5. He L, Li Y, Yang J. Theory and experiment of passive-active hybrid vibration isolation mounts using electromagnetic actuator and air spring. *Acta Acustica*, 2013, 38(2): 241-249.
6. Jin Guoyong, Zhang Hongtian. Active Control of a Two-stage Active Vibration Isolation System with Online Secondary Path Modeling, 2009, 1811-1815.
7. Tom Oomen, Rick van der Maas, Cristian R. Rojas, Håkan Hjalmarsson. Iterative Data-Driven H^∞ Norm Estimation of Multivariable Systems With Application to Robust Active Vibration Isolation, *Control Systems Technology*, 2014, 2247-2260.
8. Deng Xi-shu, Wu Yun-xin. Research on Modelling and Controlling for Active Vibration-isolation System on Testing Equipment of Stepping and Scanning Lithography, *High Density packaging and Microsystem Integration*, 2007, 1-5.